



Recycling of Glass Cullet and Glass Powder in Alkali-Activated Cement: Mechanical Properties and Alkali–Silica Reaction

Pingping He¹ · Binyu Zhang¹ · Shuqing Yang¹ · Hafiz Asad Ali¹ · Jian-Xin Lu¹ · Chi Sun Poon¹

Received: 7 August 2019 / Accepted: 20 May 2020 / Published online: 28 May 2020
© Springer Nature B.V. 2020

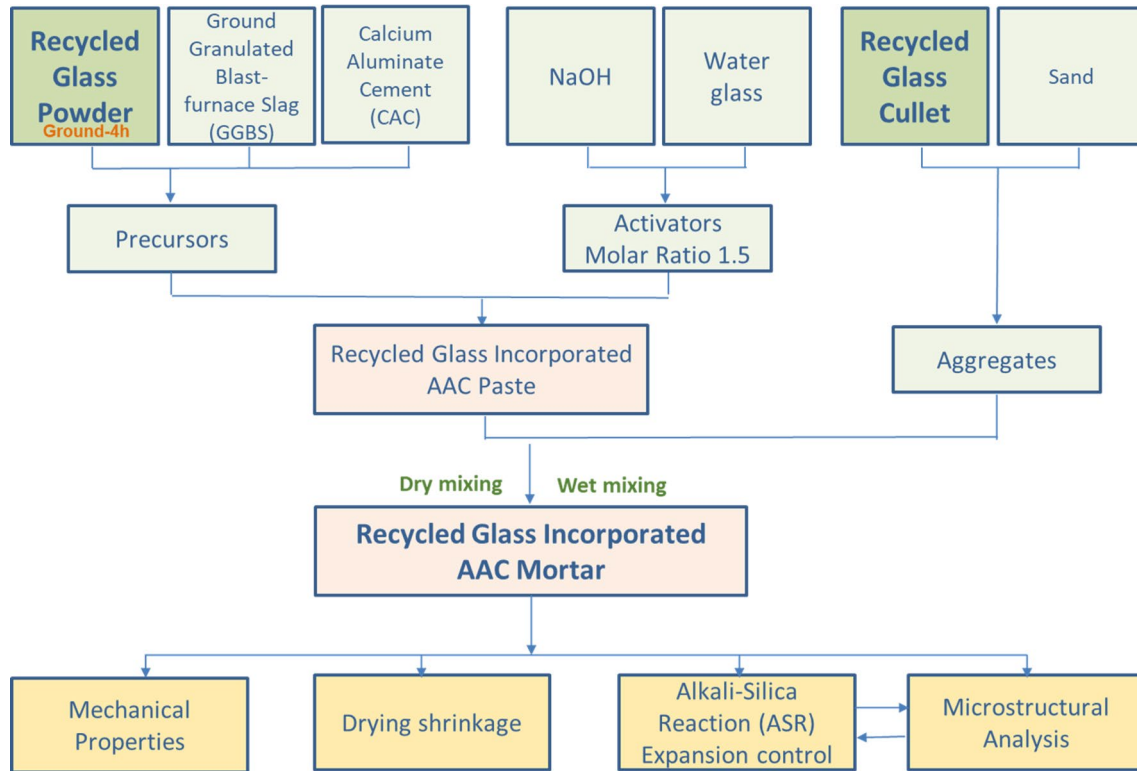
Abstract

This study investigated the compressive strength, drying shrinkage and alkali-silica reaction (ASR) expansion of alkali-activated mortars using sand or glass cullet (GC) as aggregates and using glass powder (GP) to partially replace ground granulated furnace slag (GGBS) as the precursor. For mortars using GC as the aggregate, the replacement of GGBS by GP decreased the compressive strength. The mortars using sand as aggregate showed severe drying shrinkage and the replacement of sand by GC could significantly decrease the drying shrinkage. The addition of calcium aluminium cement (CAC) could further suppress the drying shrinkage. The alkali-activated GGBS mortars using GC as the aggregate showed large expansion after alkaline immersion. When using GP to partially replace GGBS, the expansion was significantly decreased. The replacement of 15% GGBS by CAC could further decrease the expansion. The optimal alkali-activated cement (AAC) mixture proportion developed in this study was the mortars incorporating 15% of CAC, 10% of GGBS and 75% of GP as the compressive strength, expansion and drying shrinkage of this mixture could meet the stipulated mechanical and durability requirements for partition wall applications.

✉ Chi Sun Poon
cecspon@polyu.edu.hk

¹ Department of Civil and Environmental Engineering, The Hong Kong Polytechnic University, Hung Hom, Kowloon, Hong Kong

Graphic Abstract



Keywords Waste glass · Alkali-activated cement · Alkali-aggregate reaction · Calcium aluminate cement · SEM-BSE

Statement of Novelty

The manuscript provided a novel way to incorporate waste glass into AAC-based mortars. An innovative method was proposed to effectively suppress the ASR induced expansion, which is a concern associated with glass aggregates incorporation. Microstructural analysis was also conducted to reveal the mechanism behind the ASR expansion suppression.

Introduction

Waste glass is a significant solid waste type in Hong Kong due to the lack of a local glass manufacturing industry [1]. A large proportion of the waste glass is being disposed of at landfills. Due to limitations of landfill space and the environment consequences of landfilling, it is necessary to introduce practical ways to recycle waste glass. So far, ordinary Portland cement (OPC) based cement material has been considered as an effective tool for the recycling of waste glass [2–4].

Glass is a promising material for the fabrication of AAC due to its high content of Si. However, limited studies have been reported on the alkali activation of GP due to the low alkali reactivity of GP compared to other supplementary cementitious materials such as GGBS and fly ash [5].

The effect of GP content on the compressive strength of alkali-activated cement varies for different types of glasses. Some researchers found the compressive strength of AAC increased when using some types glass such as window glass, solar panel waste glass and liquid crystal glass to replace metakaolin, which might be due to the filler effect of the inert glass powder [6]. But when using other glasses, such as spent fluorescent lamps glass [7] and soda lime silicate glass [8–10], the strength of AAC decreased due to the low alkali reactivity of the glasses. Even using the same type of glass, the effect of glass content on the strength of AAC varied under different conditions, such as curing temperature, ratio of alkalis used, etc [11]. Besides, the compressive strength of the alkali-activated glass cement decreased under moist curing conditions due to the poor hydrolytic stability of sodium silicate gel [12]. The addition of GGBS or metakaolin could control the strength loss [5].

Table 1 Chemical compositions of GGBS, GP and CAC (% by mass)

	SiO ₂	CaO	AlO ₃	Na ₂ O	Fe ₂ O ₃	K ₂ O	SO ₄	MgO
GGBS	35.14	37.79	13.24	–	0.33	0.85	3.25	7.85
GP	73.29	12.14	1.10	10.54	0.30	0.84	0.24	1.25
CAC	2.65	38.76	57.03	–	0.65	0.21	0.32	0.24

Even though GP showed low AAC reactivity, it has the ability to inhibit ASR expansion in OPC based materials [13]. This might be because the addition of GP led to the decrease in the permeability of the concrete and thus leading to a reduction of the migration of alkalis towards the reactive aggregate [14]. Further research is required to verify the exact mechanism. But few studies have used GC as the fine aggregate to prepare AAC mortars or concrete as the GC might react with alkali in the pore solution and induce severe expansion and cracks [8]. Additional aluminum sources might be used to mitigate ASR expansion as it was reported that aluminum could be absorbed on the surface of alkali reactive aggregate and inhibit the dissolution of aggregates [15].

The aim of this study is to maximize the use of recycled glass in AAC mortars prepared with GC as the fine aggregate and GP as a part of the precursor. CAC was used as the replacement of GGBS to mitigate the drying shrinkage and ASR expansion.

Experimental Program

Materials

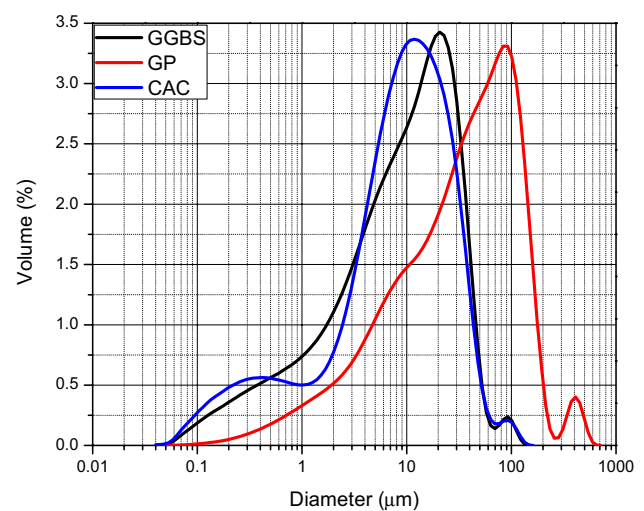
The precursors used in this study included GGBS, CAC and GP. GGBS and CAC were provided by a commercial source. A standard sand that complied with the grading requirement of ISO 679:1999 and EN196-1 was used in this study. GC was obtained from a local glass recycler who collected and recycled waste beverage bottles (soda-lime glass) to GC. Mixed coloured GC was produced by the recycler. The GP was obtained by milling recycled GC for 4 h using a laboratory ball mill. The chemical compositions of GGBS, GP and CAC are shown in Table 1. The particle size distributions of these three powders are shown in Fig. 1. The specific surface areas of GGBS, GP, and CAC were 1.5658 m²/g, 0.8947 m²/g and 1.3445 m²/g respectively. The activators were an AR grade NaOH and the water glass was composed of 28.3% SiO₂, 8.6% Na₂O and 58.4% H₂O. The gradation of GC is shown in Table 2.

Mix Design and Specimens Preparation

Table 3 shows the mix design of alkali-activated mortars. Two casting methods were used in this study: (i) wet-mix

Table 2 Particle grading of GC

Sieve size	Percentage (%)
2.36 mm–5 mm	42.4
1.18 mm–2.36 mm	22.2
0.6 mm–1.18 mm	21.4
<0.6 mm	14.1

**Fig. 1** Particle size distributions of GGBS, GP and CAC

method and (ii) dry-mix method. The compaction of traditional wet-mix samples was obtained by using a vibration table while the compaction of dry-mix samples was obtained by using a compressive load [16]. The dry-mix method is for the real induction production. The mixture proportions of the wet-mix samples and the dry-mix samples were similar, except the water/binder ratio. The water/binder ratio of 0.4 was used to obtain good workability for the wet-mix samples. The dry-mix samples used a lower water/binder ratio (0.17) to obtain a fresh mortar mixture with a zero-slump value.

The dry-mix samples were cast in two equal layers and a compaction equipment with a compressive load of 30N/mm² was used to compact the samples as described in previous literature [17]. The dry-mix samples were demolded immediately and were cured under laboratory conditions (25 °C and 75% RH) for 1 day while the wet-mix samples

Table 3 Mix design of alkali-activated mortars (by mass)

Mixtures notation	Binder (%)			Activator/Binder	GC/ Binder	Sand /Binder	Water/Binder	Modulus SiO ₂ /Na ₂ O
	GP	CAC	GGBS					
SS100	0	0	100	0.164	0	2.7	0.4	1.5
SS75G25	25	0	75	0.164	0	2.7	0.4	1.5
SS50G50	50	0	50	0.164	0	2.7	0.4	1.5
SS25G75	75	0	25	0.164	0	2.7	0.4	1.5
S100	0	0	100	0.164	2.7	0	0.4	1.5
S50G50	50	0	50	0.164	2.7	0	0.4	1.5
S25G75	75	0	25	0.164	2.7	0	0.4	1.5
S10G75	75	15	10	0.164	2.7	0	0.4	1.5
DS100	0	0	100	0.164	2.7	0	0.17	1.5
DS50G50	50	0	50	0.164	2.7	0	0.17	1.5
DS25G75	75	0	25	0.164	2.7	0	0.17	1.5
DS10G75	75	15	10	0.164	2.7	0	0.17	1.5

were demolded after one day of curing under the same laboratory conditions.

A group of fresh mixtures was cast into the 40mm*40mm*40 mm plastic molds for compressive strength test. Another group of fresh mixtures was cast into the 25mm*25mm*285 mm steel molds for ASR expansion test and drying shrinkage test. The samples for compressive strength test were cured at laboratory conditions (25 °C and 75% RH) for 28 days. The drying shrinkage of the samples were recorded in accordance with BS ISO-Part 8 [18]. The samples were immediately immersed in water (at 25 °C) after demolding for 48 h as the initial length and then placed in a chamber with a temperature of 25 ± 2 °C and a relative humidity of 50%. The measurement of ASR expansion followed the ASTM C1260 method [19]. The samples were cured in a water bath at 80 °C for another day after demolding, followed by the alkaline immersion in a 1M NaOH solution in a plastic container which was placed in the 80 °C water bath.

Test Methods

The compressive strength test was conducted using a 300 kN capacity compression testing machine with a loading rate of 0.6 MPa/s. The length changes (shrinkage and expansion) of AAC mortar bars were recorded using a calibrated dial gauge. For the microstructural test, thin slices were cut from the prism mortars, soaked in ethanol for 24 h to remove water, dried at 60 °C in a vacuumed chamber for 2 days. Then specimens were then epoxy impregnated and polished down to 0.05 µm. After dried and carbon coated, the specimens were examined in scanning electron microscopy (SEM)-backscattered electron (BSE) mode using a JEOL JSM-6490 with an energy dispersive spectra (EDX) detector.

Results and Discussion

Compressive Strength

The compressive strength of AAC mortars using sand as aggregate and different amounts of GP as the precursor after 28 days of air curing is shown in Fig. 2. When the GP content was lower than 50%, the AAC mortars using GP as the replacement of GGBS had comparable compressive strength to the GGBS mortar (SS100). The compressive strength of SS100, SS75G25, SS50G50 at 28 days was about 60 MPa. However, the compressive strength decreased significantly when the GP content was higher than 50% (SS25G75).

Figure 3 shows the compressive strength of AAC mortars using GC as aggregate and different contents of GP as precursor after 28 days of air curing. The strength of GC

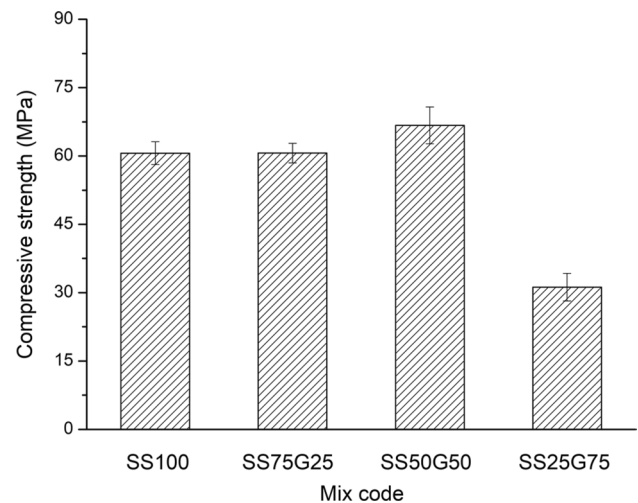


Fig. 2 Compressive strength of AAC sand mortars and different amounts of GP after 28 days of air curing

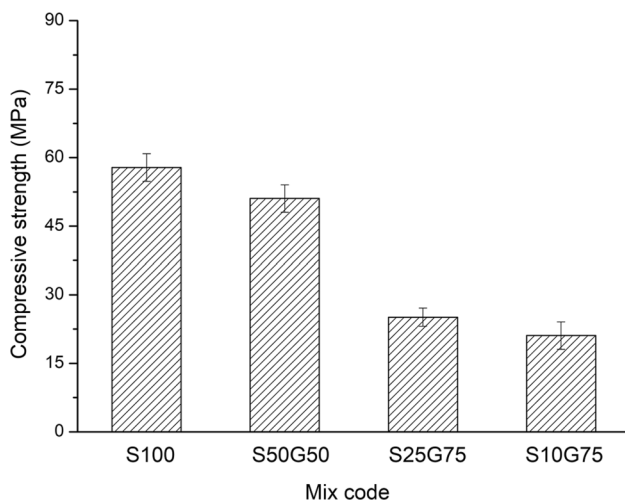


Fig. 3 Compressive strength of AAC GC mortars and different amounts of GP after 28 days of air curing

mortars was lower than that of sand mortars. Contrary to the case of using sand as the aggregate, the compressive strength of the GC mortars decreased with the increase of GP content. The AAC mortar prepared with 100% of GGBS (S100) showed the highest strength (57.5 MPa). By using 75% of GP to replace GGBS, the strength was decreased to 25.36 MPa. The compressive strength of the mortars containing 15% of CAC as the replacement of GGBS (S10G75) was lower than that of S25G75

Even though the compressive strength decreased when using GP and CAC to replace GGBS, the compressive strength of S10G75 was higher than 10 MPa after 28 days of air curing and the product could be used as partition wall blocks.

Drying Shrinkage

Figure 4 shows the effect of GP content on the drying shrinkage of AAC sand mortars at 28 days. Even though there is no standard with respect to the drying shrinkage of AAC mortars, it was suggested that the drying shrinkage value should be lower than 1000 micro strain to avoid cracking and damage to the structure [20]. From this result, it can be seen that the drying shrinkage of all the samples were much higher than 1000 micro strain. The increase of GP content led to an increase of drying shrinkage when the GP content was lower than 50%. When further increasing the GP content, the drying shrinkage decreased. However, the shrinkage value of the mortars incorporating 75% of GP (SS25G75) was still much higher than 1000 micro strain

The drying shrinkage values of AAC mortars incorporating GC as aggregate at 28 days are shown in Fig. 5. It can be seen that the drying shrinkage value was dramatically decreased. The shrinkage of the mortar using only GGBS as

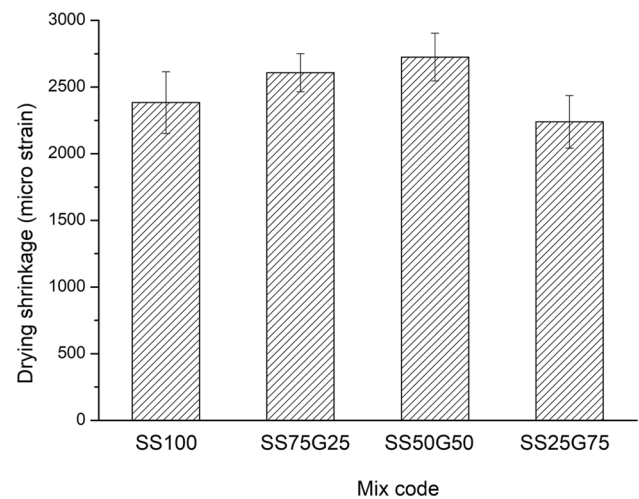


Fig. 4 Drying shrinkage of AAC sand mortars

the precursor (S100) was 873 micro strain. When using GP as the replacement of GGBS, the drying shrinkage increased. The shrinkage value of S25G75 was higher than 1000 micro strain at 28 days. The addition of CAC as a replacement of GGBS significantly decreased the drying shrinkage. The drying shrinkage of S10G75 was only 662 micro strain at 28 days. This indicates that the drying shrinkage of AAC mortars incorporating GC as the aggregate and a large amount of GP as precursor could be controlled to lower than 1000 micro strain when using CAC as the replacement of GGBS.

ASR Stability

Figure 6 shows the effect of GP content on the ASR expansion of AAC mortars using sand as the aggregate after alkaline immersion. The alkali-activated GGBS mortar (SS100)

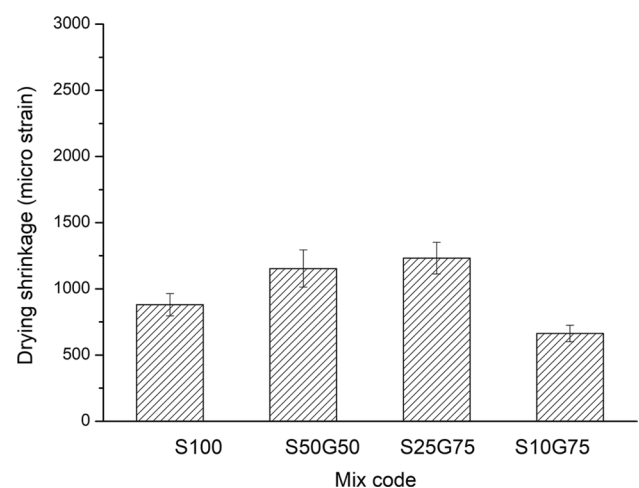


Fig. 5 Drying shrinkage of AAC GC mortars

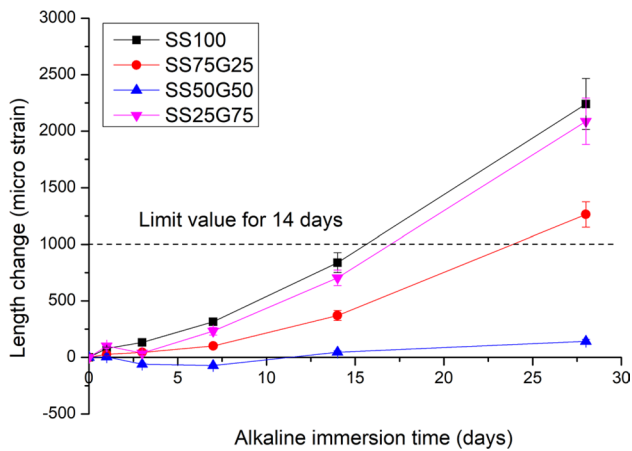


Fig. 6 Length changes of wet-mix AAC sand mortar bars

showed continuous expansion which reached around 2250 micro strain at 28 days. When using GP as the replacement of GGBS and the GP content was lower than 50%, the expansion was significantly reduced and the expansion value of SS50G50 was negligible even after 28 days of alkaline immersion. However, further increase of the GP content (S25G75) resulted in large increase in expansion. The expansion of SS25G75 was comparable to SS100 at 28 days. This indicated that the GP content in the AAC mortar should be kept at lower than 50% to control the expansion of the AAC sand mortars

Figure 7 shows the length change of AAC GC mortar bars prepared with different contents of GP as precursor after alkaline immersion. It can be seen that S100, S50G50, and S25G75 showed higher expansion values compared to the AAC sand mortars prepared with the same GP contents (Fig. 6). The alkali-activated GGBS mortar (S100)

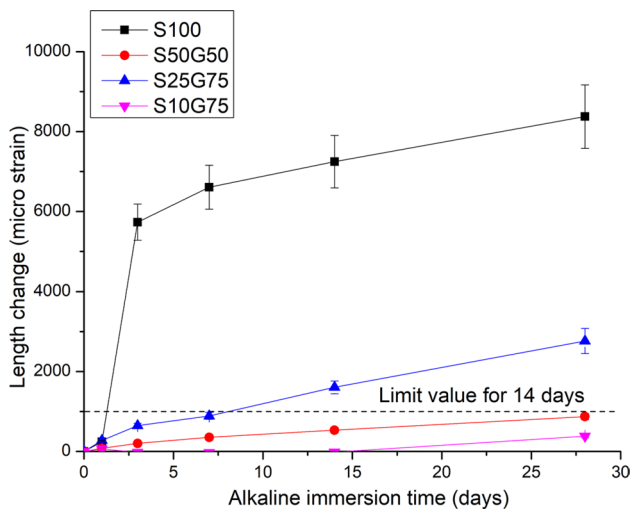


Fig. 7 Length changes of wet mix AAC GC mortar bars

expanded rapidly in the first 3 days and reached around 8300 micro strain after 28 days of alkaline immersion. Similar to the trend found in Fig. 6, the expansion was significantly reduced when GP was used to replace GGBS. The expansion of S50G50 was only 870 micro strain after 28 days of alkaline immersion. But the expansion increased when further increasing the GP content and reached around 2727 micro strain when the GP content was 75% (S25G75)

By using 15% CAC to replace the GGBS (S10G75), the expansion was significantly decreased to 378 micro strain. It indicates that CAC could significantly suppress the ASR expansion, and the expansion of AAC mortar prepared with 75% GP could be controlled to a lower value if using 15% CAC as the replacement of GGBS.

The length changes of the dry-mix AAC GC mortars are shown in Fig. 8. The initial shrinkage might be due to autogenous shrinkage [21]. The autogenous shrinkage of the dry-mix sample was much higher than that of the wet-mix sample. It was reported that the autogenous shrinkage increased with the decrease of water to binder ratio [22]. The reaction degree of the dry-mix sample might be lower than that of the wet-mix sample during steam curing due to the lower water to binder ratio. And the reaction developed fast during alkaline immersion for dry-mix sample. Therefore, the lower water to binder ratio of the dry-mix sample might result in the higher autogenous shrinkage. The most noticeable finding is the expansion of all the dry-mix mortars was lower than that of the wet-mix samples, which means the dry-mix method could suppress the ASR expansion of the AAC GC mortars. The expansion of DS100 at 28 days was around 1000 micro strain. The effect of GP content on the length change in the dry-mix samples was similar to that found in the wet-mix AAC mortars. The expansion after 28 days of alkaline immersion decreased with the increase of GP content when the GP content was lower than 50% and increased when further increasing the GP content.

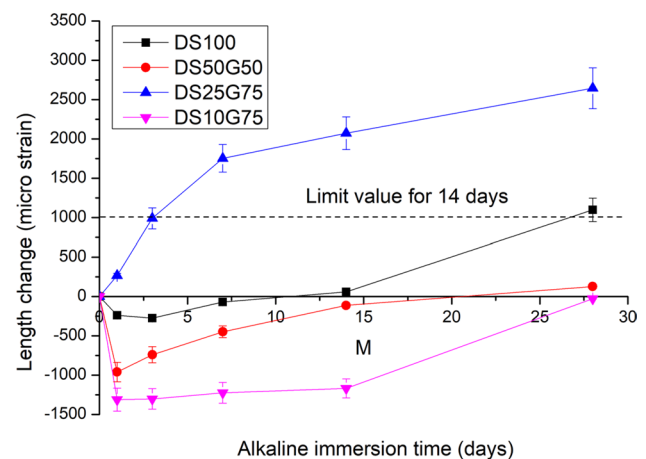


Fig. 8 Length changes of dry-mix AAC GC mortar bars

SEM-BSE Analysis

Comparison Between Wet-Mix and Dry-Mix Samples

Figure 9 presents the SEM (BSE) images of the dry-mix and the wet-mix AAC mortars using sand or GC as aggregate. From Fig. 9a–c, it can be seen that the dry-mix AAC mortars (DS25G75) had a more porous structure in contrary to the wet-mix mortars (SS25G75 and S25G75). From the images with higher magnifications (Fig. 9d–f), ASR gel was found around the GC surface but absent around the sand particles. Therefore, the absence of ASR gel might be the reason for the lower expansion of the AAC sand mortars

Effect of GP on ASR

Figure 10 shows the SEM-BSE images of the wet-mix AAC GC mortars using different contents of GP to replace GGBS as the precursor before and after alkaline immersion. After 1 day of water bath curing, a gap between GC and the paste was observed in all the mixtures which showed the poor bonding between GC and the AAC paste. For sample S100, the ASR gel firstly filled the cracks inside the glass particles. The surface of GC seems to be intact. Then the ASR

gel inside GC seems to be expanded with the prolonging of immersion time. Some ASR gel was found on the surface of GC after 14 days of immersion

When using 50% of GP to replace GGBS (S50G50), the gel-filled cracks were also observed, but the rim of ASR gel surrounding the GC was much smaller and a rim could also be clearly observed around GP which was the reaction product of GP with the alkali. When using 15% of CAC to replace GGBS (S10G75), the ASR gel rim around GC was not obvious and no ASR gel was observed in the cracks. This agrees with the length change results (Fig. 7) that the use of CAC could further decrease the expansion during alkaline immersion.

Table 4 shows the elemental compositions analysis results of ASR gel for AAC mortars after alkaline immersion for 14 days. The Ca/Na ratio of ASR gel in the cracks was slightly higher than that around GC. It was mentioned above that the GP continuously reacted during alkaline immersion and rims of gel around GP could be observed. The Ca/Na ratio of the rim around GP was higher than that of ASR gel in S50G50 or S100. The ASR gel in S10G75 had a much higher Na/Si ratio compared to the other samples. The Ca/Si ratio and Na/Si ratio might be related to the swelling characteristics of ASR gel, which will be discussed in the next section.

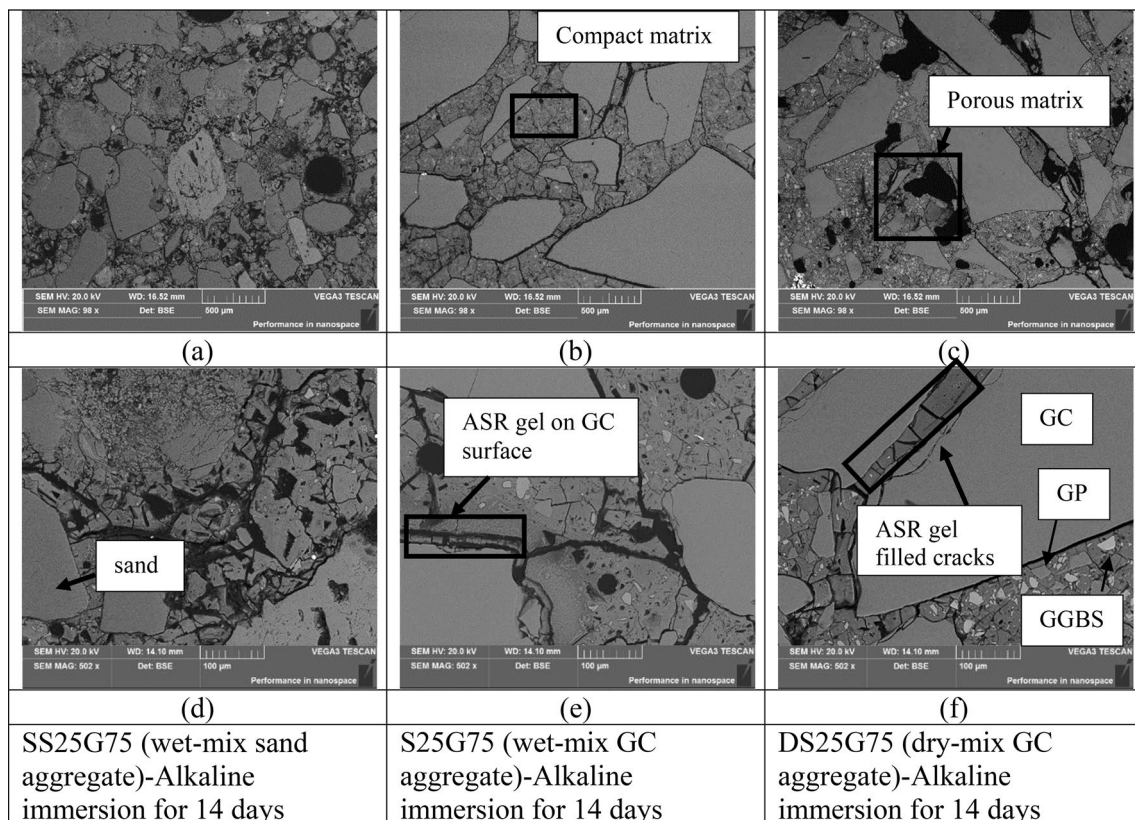


Fig. 9 SEM-BSE micrographs of wet-mix and dry-mix AAC mortars prepared with sand or GC aggregates after alkaline immersion (a–c \times 100; d–f \times 500)

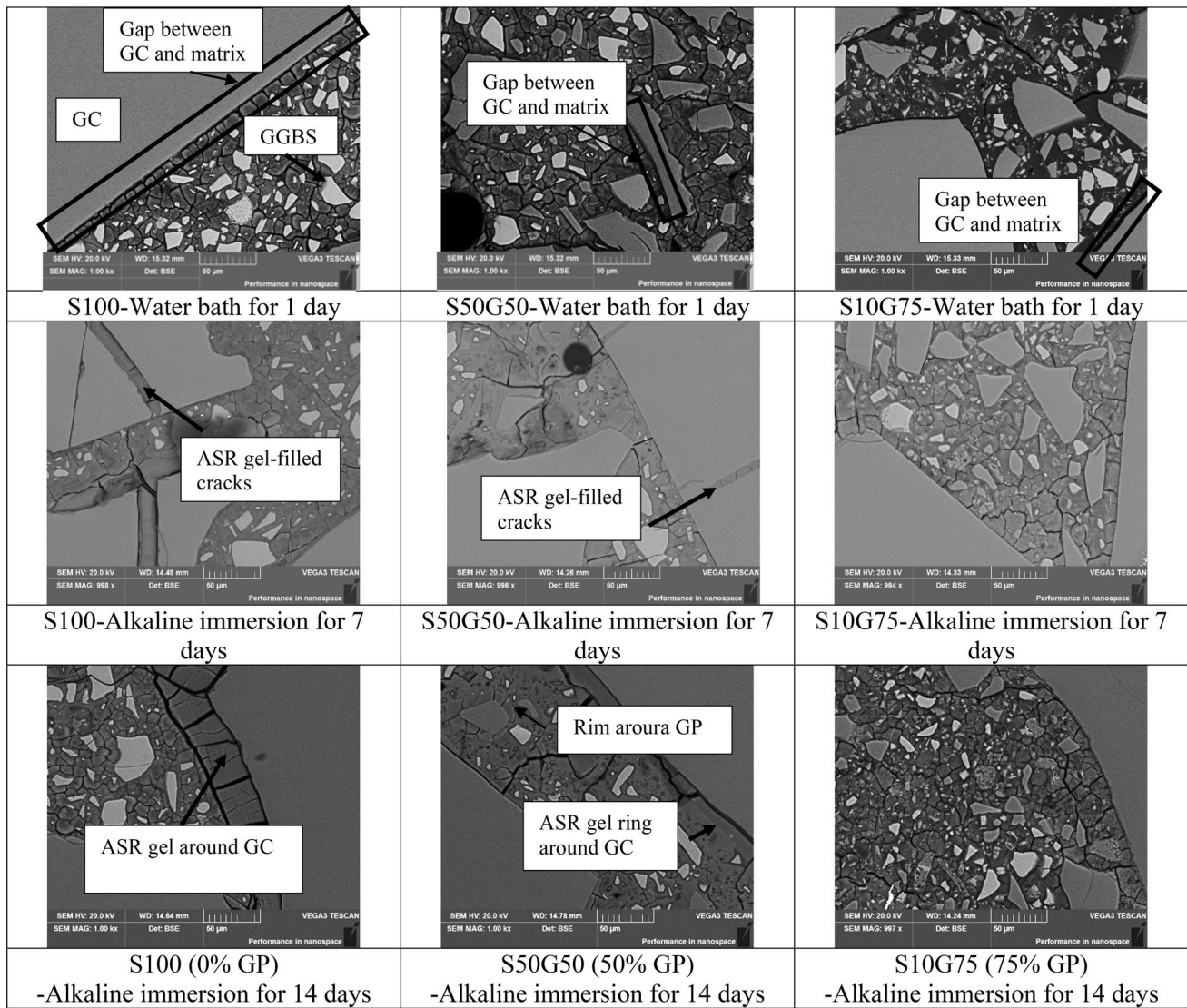


Fig. 10 SEM-BSE micrographs of AAC mortars prepared with different glass powder (GP) contents before and after alkaline immersion

Table 4 EDX analysis results of the ASR gel for the wet-mix mortar samples prepared with different GP contents after 14 days of alkaline immersion

No.	ASR gel in cracks				ASR gel around GC				Rim around GP				Expansion
	Ca/Si	Na/Si	Al/Si	Ca/Na	Ca/Si	Na/Si	Al/Si	Ca/Na	Ca/Si	Na/Si	Al/Si	Ca/Na	
S100	0.27	0.18	0.08	1.5	0.24	0.19	0.06	1.26	–	–	–	–	High
S50G50	0.24	0.22	0.06	1.09	0.19	0.18	0.03	1.06	0.31	0.22	0.10	1.58	Low
S10G75	–	–	–	–	0.22	0.23	0.06	0.96	0.27	0.18	0.05	1.55	Negligible

Discussion

The compressive strength of the GC mortars was lower than that of the sand mortars, which might be related to the smooth surface of the GC. The effect of GP as the

replacement of GGBS on the compressive strength of the sand mortars was different from that of the GC mortars. When the GP content was lower than 50%, it would not affect the strength of the AAC sand mortar [23]. However, the strength of AAC GC mortars decreased with the increase of GP content due to the lower reactivity of GP

compared to that of GGBS [24]. When the GP content was fixed at 75%, the incorporation of CAC as the replacement of GGBS could further decrease the strength of GC mortars, which might be due to the reaction product formed in this system included zeolite, and zeolite had a lower strength compared to the AAC gel [25, 26].

The SEM image showed that there was a distinct interface between GC and AAC paste due to the smooth surface of the GC. The interface might accommodate the shrinkage-induced pressure. This might be one reason why the drying shrinkage of GC mortars was much lower than that of the sand mortars. For the GC mortars and the sand mortars, the increase of GP content only resulted in a slight increase of drying shrinkage. The incorporation of CAC as the replacement of GGBS could further decrease the drying shrinkage. The effect of GP and CAC on the drying shrinkage might be related to the change of the AAC gel characteristics and the pore size distribution [27], which need further research to reveal the exact mechanism.

The GC mortars experienced much higher ASR expansion than the sand mortars when only GGBS was as the precursor, which was due to the formation and swelling of ASR gel. The incorporation of GP as the replacement of GGBS could decrease the expansion when the GP content was lower than 50%. The rim of ASR gel surrounding the GC was much smaller in the mortars containing GP than that without GP. This was because the alkali continuously reacted with GP instead with GC during alkaline immersion due to the higher reactivity of GP compared to that of GC. The smaller ASR gel rim around GC might be one reason why the GP was able to suppress the ASR expansion of the AAC glass mortars. Even though a rim around GP was observed, it might have a lower swelling capacity compared to that around GC due to the higher Ca/Na ratio [28, 29]. Besides, some researchers found that the particle size of glass affected the expansion due to ASR gel. When the particle size of glass was less than 0.5 mm or higher than 50 mm, the 14-day expansions were similar to those of the reference bars that contained no glass aggregate [30]. So, the GP particles having smaller particle sizes might not induce ASR expansion. However, further increase of GP content induced a higher ASR expansion, which might be because the alkalis released from the soda lime glass would ultimately cause ASR gel formation. Besides, the lower strength of AAC mortars containing a high content of GP might be another reason for the increase in expansion as the lower strength could not restrain the expansive stresses induced by the swelling ASR gel.

The use of CAC could further decrease the expansion during alkaline immersion. The ASR gel rim around GC was not obvious and no ASR gel was observed in the cracks. This might be related to two reasons. Firstly, the CAC could react with alkali in the pore solution forming zeolite [31], thus the alkalinity of pore solution decreased and resulted in a

lower ASR expansion. Secondly, the ASR gel in the mortars containing CAC had a lower viscosity due to the higher Na/Si ratio, thus the pressure induced by the ASR expansion could be easily relieved to the surrounding pores [32, 13].

The dry-mix samples showed much lower ASR expansion compared to the wet-mix samples. The crushing of the glass bottle into aggregates produced a lot of initial cracks. In the wet-mix samples, as the expansion of ASR gel was first formed in the newly formed cracks, the propagation of cracks led to higher ASR expansion. But for the dry-mix samples, because of the presence of larger pores in the AAC matrix caused by the poorer distribution of the solid particles, ASR gel was mainly observed on the surface of the glass aggregates in the large pores, although a lesser amount was also detected in the initial internal cracks. Therefore, the large pores in the dry-mix samples could partially relieve the ASR gel expansion and the samples experienced lesser expansion compared to the wet-mix samples [33, 17].

The ASR gel was found on the surface of GC in the wet-mix AAC mortars. This phenomenon was different from that in the OPC GC mortars. It was reported that the glass-paste interface was clean and ASR gel was not observed on the GC surface after 30 days of alkaline immersion in the OPC GC mortar. This was attributed to the presence of $\text{Ca}(\text{OH})_2$ at the glass-cement paste interface which could favor the formation of CSH and prevent the formation of ASR gel [34]. $\text{Ca}(\text{OH})_2$ was absent in the wet-mix AAC mortars. Therefore, the ASR gel was observed on the surface of GC. This study developed a new way to recycle waste GC in AAC mortars. The comparison of properties between AAC GC mortar and OPC GC mortar need further research.

Conclusions

Based on the above results and discussion, the conclusions of this study are summarized as follows:

- (1) The sand mortars showed higher compressive strength than the GC mortars. The replacement of GGBS by GP would not decrease the compressive strength of the sand mortars. However, the use of GP decreased the strength of GC mortars. The compressive strength of the alkali-activated slag mortar was 57.5 MPa after 28 days of air curing, while the strength of the mortars incorporating 75% of GP was 25.36 MPa at 28 days. The use of CAC further decreased the compressive strength. But the strength was higher than 10 MPa at 28 days when using 15% of CAC and 75% of GP as the replacement of GGBS, which means this product could be used as partition wall blocks.
- (2) The mortars prepared by using sand as the aggregate showed severe drying shrinkage. The replacement of

sand by GC could decrease the drying shrinkage. The drying shrinkage of the alkali-activated slag mortars using GC as aggregate was 873 micro strain at 28 days. The replacement of GGBS by GP increased the drying shrinkage. And the shrinkage of AAC mortars incorporating 75% of GP and 25% of GGBS was higher than 1000 micro strain. The use of CAC decreased the drying shrinkage of the mortars. When using 15% of CAC and 75% GP, the drying shrinkage of the mortars was only 662 micro strain at 28 days.

- (3) When using GC as aggregates, the alkali-activated slag mortars showed much higher expansion compared to the sand mortars due to the formation of ASR gel. The expansion of GC mortars reached around 7750 micro strain after 28 days of alkaline immersion.
- (4) The use of GP as a replacement of GGBS could significantly decrease the ASR expansion when the GP content was lower than 50%. The expansion of AAC GC mortars prepared with 50% of GP and 50% of GGBS was only 870 micro strain after 28 days of alkaline immersion. The ASR expansion suppression of GP might be attributed to that the GP showed a lower reactivity compared to GGBS. The alkali would react with GP instead of GC during alkaline immersion. Therefore, the reaction between alkali and GC was reduced. When the GP content was higher than 50%, the expansion of GC mortars increased, which might be due to the sodium released from the GP.
- (5) Even though the mortars prepared with 75% of GP and 25% of GGBS had a high ASR expansion, the addition of CAC as the replacement of GGBS could significantly decrease the ASR expansion. When using 15% CAC as the replacement of GGBS, the expansion was only 378 micro strain at 28 days of alkaline immersion. This might be related to the ASR gel formed in the CAC-blended AAC mortars had a lower viscosity due to the higher Na/Si.
- (6) The mortars prepared with the dry-mix method showed lower expansion compared to the wet-mix samples because the higher porosity in the dry-mix samples could accommodate the expansion pressure.

Acknowledgements The authors wish to acknowledge the financial support of the Environment and Conservation. Fund of the Hong Kong SAR Government and The Hong Kong Polytechnic University.

References

1. HK EPD, Monitoring of Solid Waste in Hong Kong: Waste Statistics for 2016. Environmental Protection Department, Hong Kong (2017)
2. Kou, S., Poon, C.: Properties of self-compacting concrete prepared with recycled glass aggregate. *Cem. Concr. Compos.* **31**(2), 107–113 (2009)
3. Lu, J., Duan, Z., Poon, C.S.: Combined use of waste glass powder and cullet in architectural mortar. *Cem. Concr. Compos.* **82**, 34–44 (2017)
4. Shao, Y., Lefort, T., Moras, S., Rodriguez, D.J.C.: Studies on concrete containing ground waste glass. *Cem. Concr. Res.* **30**(1), 91–100 (2000)
5. Redden, R., Neithalath, N.: Microstructure, strength, and moisture stability of alkali activated glass powder-based binders. *Cem. Concr. Compos.* **45**, 46–56 (2014). <https://doi.org/10.1016/j.cemconcomp.2013.09.011>
6. Ogundiran, M.B., Winjobi, F.A.: The potential of binary blended geopolymer binder containing Ijero-Ekiti calcined kaolin clay and ground waste window glass. *Afr. J. Pure Appl. Chem.* **9**(7), 159–166 (2015)
7. Bobirić, C., Shim, J.-H., Pyeon, J.-H., Park, J.-Y.: Influence of waste glass on the microstructure and strength of inorganic polymers. *Ceram. Int.* **41**(10), 13638–13649 (2015)
8. Lu, J.X., Poon, C.S.: Use of waste glass in alkali activated cement mortar. *Constr. Build. Mater.* **160**, 399–407 (2018)
9. He, P., Zhang, B., Lu, J.-X., Poon, C.S.: A ternary optimization of alkali-activated cement mortars incorporating glass powder, slag and calcium aluminate cement. *Constr. Build. Mater.* **240**, 117983 (2020)
10. Zhang, B., He, P., Poon, C.S.: Optimizing the use of recycled glass materials in alkali activated cement (AAC) based mortars. *J. Clean. Prod.* **255**, 120228 (2020)
11. Martinez-Lopez, R., Escalante-Garcia, J.I.: Alkali activated composite binders of waste silica soda lime glass and blast furnace slag: strength as a function of the composition. *Constr. Build. Mater.* **119**, 119–129 (2016)
12. Torres, J., Palacios, M., Hellouin, M., Puertas, F.: Alkaline chemical activation of urban glass wastes to produce cementitious materials. In: Proceedings of the 1st Spanish National Conference on Advances in Materials Recycling and Eco-Energy Madrid, pp. 12–13. Citeseer (2009)
13. Idir, R., Cyr, M., Tagnit-Hamou, A.: Use of fine glass as ASR inhibitor in glass aggregate mortars. *Constr. Build. Mater.* **24**(7), 1309–1312 (2010). <https://doi.org/10.1016/j.conbuildmat.2009.12.030>
14. Idir, R., Cyr, M., Tagnit-Hamou, A.: Use of fine glass as ASR inhibitor in glass aggregate mortars. *Constr. Build. Mater.* **24**, 1309–1312 (2010). <https://doi.org/10.1016/j.conbuildmat.2009.12.030>
15. Bickmore, B.R., Nagy, K.L., Gray, A.K., Brinkerhoff, A.R.: The effect of Al(OH)₄⁻ on the dissolution rate of quartz. *Geochim. Cosmochim. Acta* **70**(2), 290–305 (2006)
16. Ling, T.-C., Poon, C.-S.: Use of recycled CRT funnel glass as fine aggregate in dry-mixed concrete paving blocks. *J. Clean. Prod.* **68**, 209–215 (2014). <https://doi.org/10.1016/j.jclepro.2013.12.084>
17. Yang, S., Cui, H., Poon, C.S.: Assessment of in-situ alkali-silica reaction (ASR) development of glass aggregate concrete prepared with dry-mix and conventional wet-mix methods by X-ray computed micro-tomography. *Cem. Concr. Compos.* **90**, 266–276 (2018)
18. BS ISO 1920-8, Determination of Drying Shrinkage of Concrete for Samples Prepared in the Field or in the Laboratory, British Standard Institution, UK (2009)
19. ASTM: C1260: Standard test method for potential alkali reactivity of aggregates (mortar-bar method). American Society of Testing Materials (2007)
20. AS-1012: 13, Methods of testing concrete; Method 13: Determination of the Drying Shrinkage of the Concrete Samples Prepared in

- the Field or in the Laboratory. Standards Australia International Ltd, Sydney (1992)
21. Fernández-Jiménez, A., Puertas, F.J.C.: The alkali–silica reaction in alkali-activated granulated slag mortars with reactive aggregate. *Cem. Concr. Res.* **32**(7), 1019–1024 (2002)
 22. Zhang, M., Tam, C., Leow, M.: Effect of water-to-cementitious materials ratio and silica fume on the autogenous shrinkage of concrete. *Cem. Concr. Res.* **33**(10), 1687–1694 (2003)
 23. Maraghechi, H., Salwocki, S., Rajabipour, F.: Utilisation of alkali activated glass powder in binary mixtures with Portland cement, slag, fly ash and hydrated lime. *Mater. Struct.* **50**(1), 16 (2017)
 24. Özkan, O., Yüksel, I.: Studies on mortars containing waste bottle glass and industrial by-products. *Constr. Build. Mater.* **22**(6), 1288–1298 (2008)
 25. Takeda, H., Hashimoto, S., Yokoyama, H., Honda, S., Iwamoto, Y.: Characterization of zeolite in zeolite-geopolymer hybrid bulk materials derived from kaolinitic clays. *Materials* **6**(5), 1767–1778 (2013)
 26. De Silva, P., Sagoe-Crenstil, K.: Medium-term phase stability of Na₂O–Al₂O₃–SiO₂–H₂O geopolymer systems. *Cem. Concr. Res.* **38**(6), 870–876 (2008)
 27. Collins, F., Sanjayan, J.G.: Effect of pore size distribution on drying shrinking of alkali-activated slag concrete. *Cem. Concr. Res.* **30**(9), 1401–1406 (2000)
 28. Monteiro, P., Wang, K., Sposito, G., Dos Santos, M., de Andrade, W.P.: Influence of mineral admixtures on the alkali-aggregate reaction. *Cem. Concr. Res.* **27**(12), 1899–1909 (1997)
 29. Struble, L.J., Diamond, S.: Swelling properties of synthetic alkali silica gels. *J. Am. Ceram. Soc.* **64**(11), 652–655 (1981)
 30. Bažant, Z.P., Zi, G., Meyer, C.: Fracture mechanics of ASR in concretes with waste glass particles of different sizes. *J. Eng. Mech.* **126**(3), 226–232 (2000)
 31. He, P., Zhang, B., Lu, J.-X., Poon, C.S.: ASR expansion of alkali-activated cement glass aggregate mortars. Submitted to *Construction and Building Materials*
 32. Helmuth, R., Stark, D., Diamond, S., Moranville-Regourd, M.: Alkali-silica reactivity: an overview of research. *Contract* **100**, 202 (1993)
 33. Yang, S., Poon, C.S., Ling, T.C.: Distribution of ASR gels in conventional wet-mix glass mortars and mechanically produced dry-mix glass blocks Submitted to *Construction and Building Materials*
 34. Rajabipour, F., Maraghechi, H., Fischer, G.: Investigating the alkali-silica reaction of recycled glass aggregates in concrete materials. *J. Mater. Civ. Eng.* **22**(12), 1201–1208 (2010)

Publisher's Note Springer Nature remains neutral with regard to jurisdictional claims in published maps and institutional affiliations.